Int J Thermophys
DOI 10.1007/s10765-015-1983-3

Thermal Expansion and Electrical Resistivity Studies of Nickel and ARMCO Iron at High Temperatures

D. K. Palchaev[1] · Zh. Kh. Murlieva[1] · S. H. Gadzhimagomedov[1] · M. E. Iskhakov[1] · M. Kh. Rabadanov[1] · I. M. Abdulagatov[2,3]

Received: 18 May 2015 / Accepted: 5 October 2015

Abstract The electrical resistance, $\rho(T)$, and thermal expansion coefficient, $\beta(T)$, of nickel and ARMCO iron have been simultaneously measured over a wide temperature range from (300 to 1100) K. The well-known standard four-probe potentiometric method was used for measurements of the electrical resistance. The thermal expansion coefficient was measured using the quartz dilatometer technique. Both techniques were combined in the same apparatus for simultaneous measurements of the electrical resistance and TEC for the same specimen. The combined expanded uncertainty of the electrical resistance and thermal expansion coefficient measurements at the 95 % confidence level with a coverage factor of $k = 2$ is estimated to be 0.5 % and (1.5 to 4.0) %, respectively. The distinct $\rho(T)$ scattering contribution (phonon ρ_{ph}, magnetic ρ_m, and residual ρ_S) terms were separated and extracted from the measured total resistivity. The physical nature and details of the temperature dependence of the electrical resistance of solid materials and correct estimations of the contributions of various scattering mechanisms to the measured total resistivity were discussed in terms of the anharmonic effect. We experimentally found simple, universal, physically based, semi-empirical linear correlations between the kinetic coefficient (electrical resistance) and a thermodynamic (equilibrium) property, the thermal expansion coefficient, of solid materials. The developed, physically based, correlation model has been successfully applied for nanoscale materials (ferromagnetic nickel nanowire). A new s-d-exchange interaction energy determination technique has been proposed.

✉ I. M. Abdulagatov
ilmutdin@boulder.nist.gov

1 Dagestan State University, Gadzhieva Str. 43-A, Makhachkala, Russia 367000

2 Institute of Physics of the Dagestan Scientific Center of the Russian Academy of Sciences, M. Yaragskogo Str. 94, Makhachkala, Dagestan, Russia 367005

3 Present Address: Applied Chemicals and Materials Division, National Institute of Standards and Technology, 325 Broadway, Boulder, CO 80305-3337, USA

Published online: 23 October 2015

Keywords Ferromagnetic · Magnetic contribution · Nickel · Resistivity · Thermal expansion · s-d-exchange energy

1 Introduction

The electrical resistivity (ER) and thermal expansion coefficient (TEC) of materials are complex functions of temperature. The temperature dependence of the electrical resistivity, $\rho(T)$, of ferromagnetic metals is determined by various contributions to the scattering of electrons by elementary excitations, namely, the atomic and magnetic subsystems. Taking into account the anharmonic effect allows correct estimation of the contribution of the phonon scattering, $\rho_{\mathrm{ph}}(T)$, to the measured total resistance, $\rho(T)$, both in bulk and in nanoscale materials, and enables understanding of the physical nature and details of the temperature dependence of the s-d-exchange interaction energy. The electrical resistance and TEC, $\beta(T)$, of nickel and Armco iron have been studied previously by many authors over a wide temperature range including near the critical point (Curie temperature), see below Sect. 1.1. However, as will be shown below, large scatter and inconsistencies, up to (20 to 25) % and more between the various reported TEC and ER data, were found for nickel and Armco iron. An especially large discrepancy, up to (25 to 35) % between the reported TEC data, was found near the phase transition temperature. Moreover, most reported TEC and ER data for nickel and Armco iron were published a long time ago (1970 to 1980). In our previous series of publications [1–5], we have developed the theory of the relation between the TEC and ER of solids. To verify the physical basis of the theory, accurate and consistent TEC and ER data are needed. Unfortunately, the available TEC and ER data have been obtained by different authors for different purity samples in the various laboratories. Thus, the discrepancy and inconsistency between the various TEC and ER data sources and their large uncertainties do not allow to verification of the theoretically derived relation between the TEC and ER. This allows a clear understanding of the physical basis of the relationship between the electrical resistivity (kinetic properties) and the TEC (equilibrium thermodynamic properties) of the materials at the microscopic level. Thus, the main goal of the present work is to provide simultaneous measurements of both the TEC and ER of nickel and Armco iron in the same experiment for the same purity sample. The other purposes of the present work are: (1) to develop a new technique for separation and extraction of the three distinct $\rho(T)$ scattering contributions (ρ_{ph}, ρ_{m}, ρ_{S}) from the measured total resistivity; (2) to determine the features of the energy spectrum of the oscillations of the magnetic subsystem; (3) to determine the cross section of the electron scattering; (4) to study the temperature dependence of the s-d-exchange interaction energy; and (5) to study nanoscale material (nanowire, films, nanoparticles, etc.) properties.

1.1 Review of Previous Studies

Experimentally, low- and high-temperature TEC and ER of nickel and Armco iron have been studied by many authors (see Table 1). However, most measurements were made years ago, except for a recent publication by Abdullaev et al. [6] for TEC and

Table 1 Summary of experimental electrical resistivity (ρ) and TEC (β) data of nickel and Armco iron

First author	Reference	Property	Temperature (K)	Method	Uncertainty (%)	Purity (mass %)
Nickel						
Kollie	[8]	TEC (β)	300–1000	FQD	0.8	99.965
Novikova[a]	[9]	TEC (β)	20–1700	n/a	1.5	99.98
						99.997
Abdullaev	[6]	TEC (β)	145–1615	D	1.0 to 2.5	99.98
Arbuzov	[10]	TEC (β)	373–973	D	2	99.93
Tanji	[11]	TEC (β)	273–1073	DD	n/a	99.98
Altman	[12]	TEC (β)	20–300	n/a	0.03β	99.60
Gurevich	[13]	TEC (β)	300–850	AD	n/a	
White	[14]	TEC (β)	4–283	TTC	n/a	99.99
Palchaev	This work	TEC (β)	310–1100	QD	1.4– 4.0	99.99
Kamalakar	[7]	ER (ρ)	1.05–1500	FPM	(2 ppm) 0.3	99.999
Kamalakar	[32]	ER (ρ)	4–675	FPM	(2 ppm) 0.3	99.999
Bel'skaya[a]	[15,25,26]	ER (ρ)	200–1500	PM	1.2–2.0	99.98
Shmatko	[22]	ER (ρ)	73.3–1173	n/a	n/a	n/a
Wycisk	[23]	ER (ρ)	296–1403	n/a	n/a	n/a
Laubitz	[24]	ER (ρ)	90–1250	CPM	0.2 to 0.5	99.999
Zverev	[27]	ER (ρ)	293–1673	CPM	n/a	99.81
Powell	[20,28]	ER (ρ)	293–1323	LFM	n/a	99.95
Palchaev	This work	ER (ρ)	310–1100	FPP	0.5	99.99
Armco iron						
Laubitz	[16]	TEC (β)	323–1373	n/a	10	99.83
Novikova[a]	[9]	TEC (β)	20–1700	n/a	1.3	99.98
						99.9996
White	[14]	TEC (β)	3–283	TTC	n/a	99.95
Palchaev	This work	TEC	331–1042	QD	1.4–4.0	99.98
Shanks	[17]	ER (ρ)	1–1273	FPP	0.5	99.52
Laubitz	[16]	ER (ρ)	273–1273	CPM	1.0–1.5	99.83
Gumenuk	[18]	ER (ρ)	293–1723	CPM	1.5 (abs.)	99.98
Watson	[19]	ER (ρ)	78–1653	SCSR	0.1 to 0.8	99.83
Powell	[20,28]	ER (ρ)	273–1300	LFM	n/a	99.92
Fulkerson	[21]	ER (ρ)	4–1273	PM	0.3	99.50
						99.95
Oleinikov	[29]	ER (ρ)	293–973	n/a	1.3	99.95
Palchaev	This work	ER (ρ)	331–1042	FPP	0.5	99.98

FPP four-probe potentiometric method, *PM* potentiometric method, *FQD* fused-quartz dilatometer, *QD* quartz dilatometer method, *DD* differential dilatometer, *D*-dilatometer (DIL-402C), *AD* automated dilatometer, *LFM* longitudinal-flow method, *PM* potentiometric method, *FPM* four-probe method, *CPM* compensation (potentiometric) method, *TTC* three-terminal capacitance technique, *SCSR* series calibrated standard resistors

[a] Reference data (recommended data)

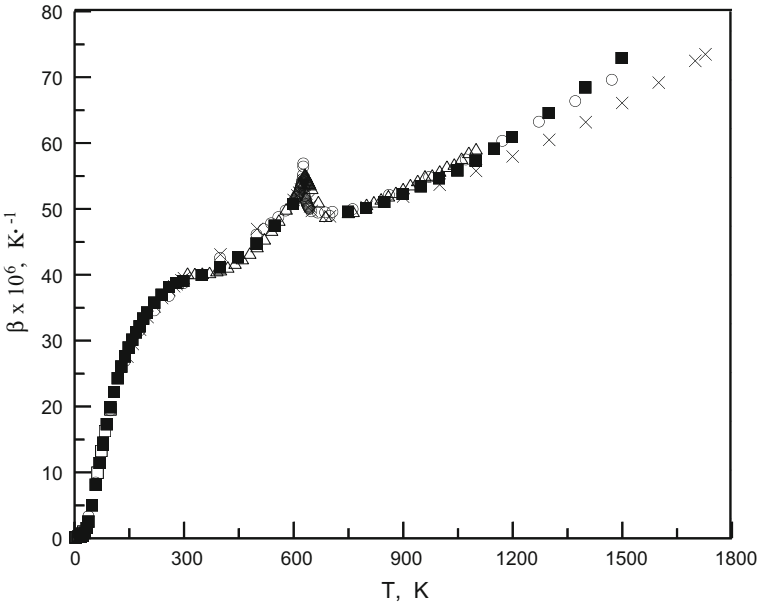

Fig. 1 Measured TEC of nickel as a function of temperature together with reported data. ◯—Kollie [8]; △—this work; ■—Novikova [9]; ×—Abdullaev et al. [6]; □—White [14]

ER measurements by Kamalakar [7]. A summary of selected, most reliable literature data for TEC [6,8–14] and ER [7,15–29] of nickel and Armco iron is given in Table 1. More than 12 datasets for the TEC and 14 for ER are included in the table. In this table, the references to original experimental data are given together with the experimental temperature range for each study. The purity, methods, and the uncertainty claimed by the authors are also included in the table. The selected, most reliable reported experimental TEC and ER data for nickel and Armco iron are given in Figs. 1, 2, 3, 4, 5, and 6 together with the present measurements. These figures show the typical temperature dependence of the TEC and ER of solid materials in a wide temperature range (from 1 K to 1653 K) including the phase transition point. The typical uncertainty of the measured TEC and ER claimed by the authors is within (1 to 4) % and (0.5 to 1.5) %, respectively. Several methods (see Table 1) such as (1) the quartz dilatometer method; the differential dilatometer; the capacitance method; the interferometric principle for TEC measurements and (2) the four-probe potentiometric method; the longitudinal-flow method; and the compensation (potentiometric) method for ER measurements have been applied for accurate determination of the TEC and ER of nickel and Armco iron over a wide temperature range. Below, we give a brief review of some of the studies that report TEC and ER data for nickel and Armco iron.

1.1.1 Thermal Expansion Coefficient

As one can see from Figs. 1 and 4, a large scatter (within 20 % and more) of the reported TEC data was observed for nickel and Armco iron. An especially large discrepancy,

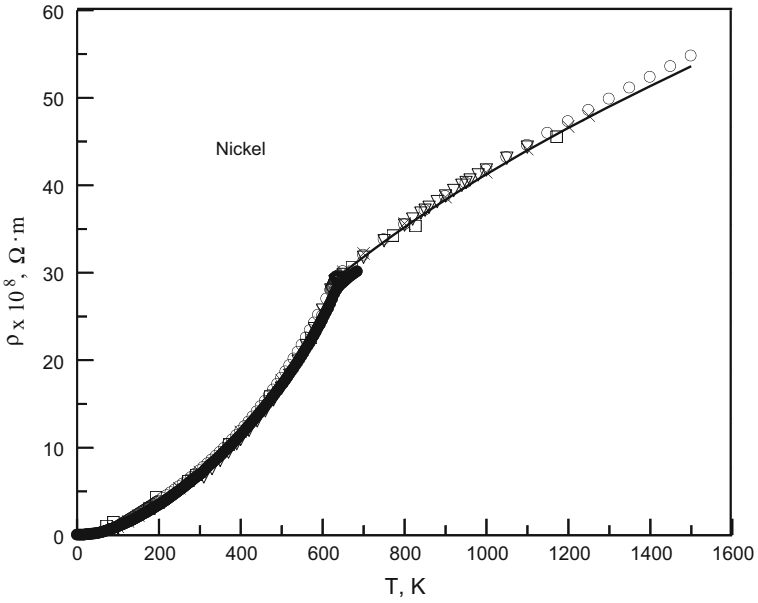

Fig. 2 Measured electrical resistivities of nickel as a function of temperature together with reported data. •—Kamalakar [7]; ◯—Bel'skaya and Peletsky [15,25]; □—Shmatko and Usov [22]; ×—Laubitz et al. [24]; ▽—this work. *Solid line* is calculated from correlation by Bel'skaya and Peletskii [15]

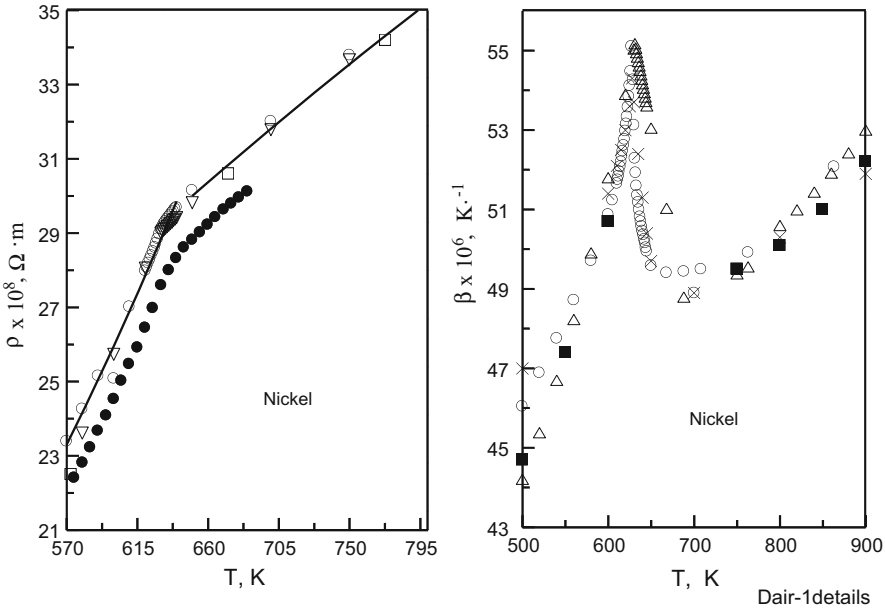

Fig. 3 Detailed view of the reported electrical resistivity (*left*) and TEC (*right*) measurements of nickel as a function of temperature near the phase transition temperature. The (*symbols*) are the same as in Figs. 1 and 2

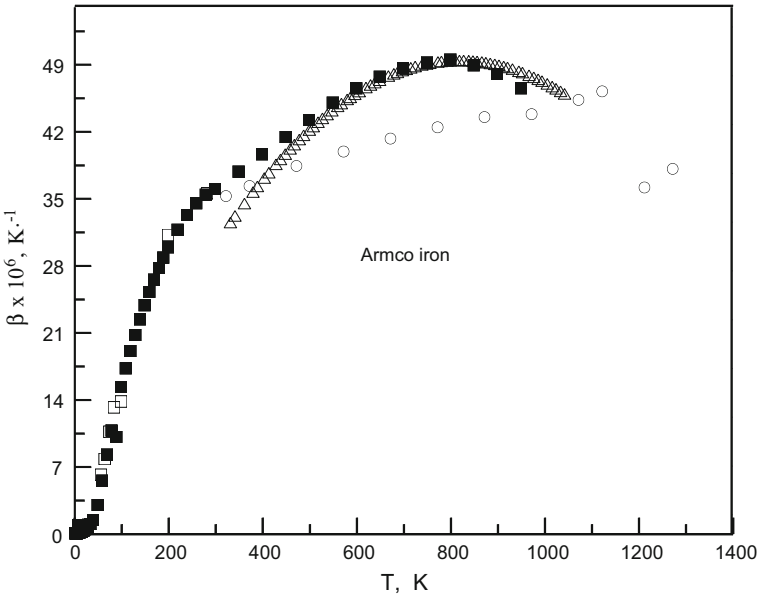

Fig. 4 Measured TEC of Armco iron as a function of temperature together with reported data. ◯—Laubitz [16]; △—this work; ■—Novikova [9]; □—White [14]

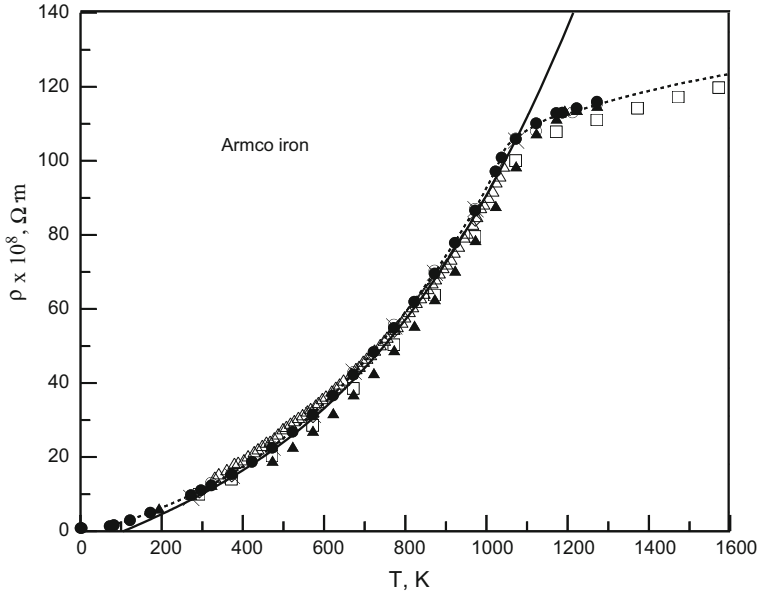

Fig. 5 Measured electrical resistivities of Armco iron as a function of temperature together with reported data. •—Shanks et al. [17]; ◯—Laubitz [16]; □—Gumenuk and Lebedev [18]; △—this work; ▲—Fulkerson et al. [21]; ×—Powell et al. [20,28]; ◇—Oleinikov [29]. *Solid line* calculated from correlation by Arajs and Colvin [31]. *Dashed line* is NIST reference data, Watson et al. [19].

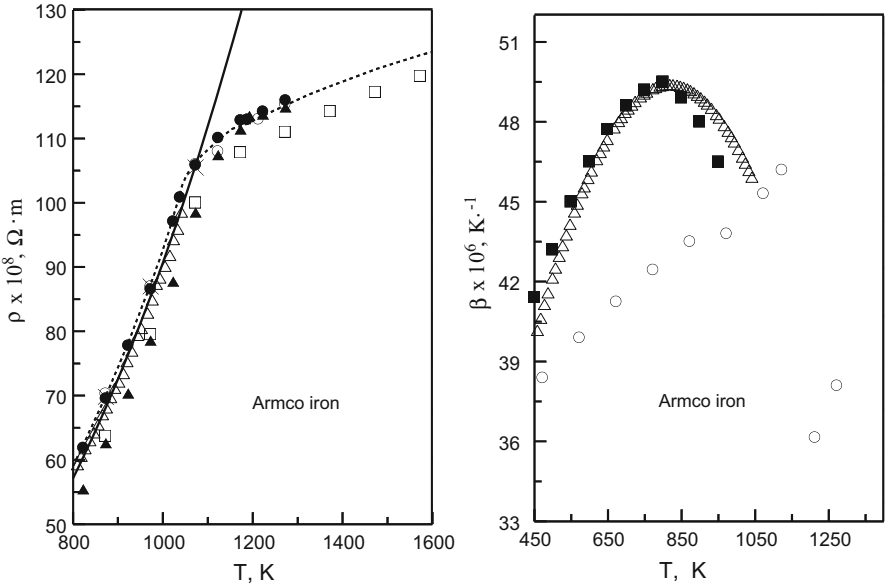

Fig. 6 Detailed view of the reported electrical resistivity (*left*) and TEC (*right*) measurements of Armco iron as a function of temperature near the phase transition temperature. The (*symbols*) are the same as in Figs. 4 and 5

up to (20 to 25) % between the reported TEC data, was found near the phase transition temperature (see detailed view in Figs. 3, 6). As was mentioned in a recent publication by Abdullaev et al. [6], although the TEC of nickel has been measured for a long time by many authors, there is still a large disagreement between the various reported data. The present detailed critical analysis of the reported TEC data for nickel showed that there is a large discrepancy (about 10 % to 30 %) between various reported datasets, especially near the Curie temperature and high temperatures (above 850 K), see also [8,9]. Various authors used different purity samples which considerably affected the accuracy of the measurements, especially near T_C . Recently, Abdullaev et al. [6] reported TEC data for nickel (99.98 mass %) over the temperature range from (145 to 1615) K. The measurements were performed using the dilatometer method. The uncertainty of the measurements is (1.0 to 2.5) %. These data are in an acceptable agreement with the data reported by Arbuzov and Zelenskii [10] and by Tanji [11]. The deviations are within (1 to 3) % at high temperatures (above 700 K) and (5 to 7) % at low temperatures (in the paramagnetic phase). Good agreement (deviations less than 0.5 %) was observed between the data by Abdullaev et al. [6] and the measurements by Altman et al. [12] at low temperatures (below room temperature). For most reported TEC data for nickel, large discrepancies were observed at temperatures from room temperature to T_C due to the sample purity and microstructural characteristics. Kollie [8] used the fused-quartz differential dilatometer to measure the TEC of nickel (purity of 99.965 mass %) in the temperature range from (300 to 1000) K. The accuracy of the method was established by measurements on standards certified by NIST. By combining these 291 data points with selected low- and high-temperature data from

the literature, values of the TEC were compiled for temperatures between (0 and 1500) K. These data together with the present and other reported data are presented in Figs. 1 and 3 (right). The uncertainty of the measurements is 0.8 %. The TEC data of nickel reported by Kollie [8] deviate from the 34 previously reported data sources within (5 to 6) % which is three times larger than the combined uncertainty of 1.8 %. Good agreement within 2 % was found between the present TEC measurements for nickel and the reported data by Kollie [8] and recent measurements of Abdullaev et al. [6] near the Curie temperature. At high temperatures (above the Curie temperature, $T > 1100$ K), recent reported data by Abdullaev et al. [6] systematically lower than the present results and the data of Kollie [8] by (5 to 10) %. Three TEC datasets [8,9] and the present results agree in over the whole measured temperature range within (2 to 3) %. Novikova [9] compiled their own measured TEC data for nickel with other critically analyzed data from the literature in the temperature range from (20 to 1700) K. These data were accepted as the recommended Russian reference TEC data for nickel. In general, most reported low-temperature TEC measurements of nickel are in good agreement with each other while, at high temperatures, the discrepancy of the reported data reaches up to 20 % and more, especially around the critical temperature.

The deviations of the present TEC data for Armco iron from the reported reference data by Novikova [9] are within 3 % while the data by Laubitz [16] show deviations up to 15 % near the phase transition temperature and (3 to 4) % at room temperature. Laubitz [16] measured the TEC of Armco iron (99.83 mass %) over the temperature range from (273 to 1273) K with a very low uncertainty of 10 % (see Figs. 4, 6). Good agreement, within their experimental uncertainty (1.5 to 2.0) %, has been observed between the present results and the measurements by Arbuzov and Zelenskii [10].

1.1.2 Electrical Resistivity Data

The measured ER data of nickel [25] together with the previous reported data of ten sources were compiled by Bel'skaya and Peletsky [15,26]. The purity and uncertainty of the previous measured samples was less than 0.8 mass % and (1 to 2) %, respectively. Most previous measurements of the ER for nickel were made using the compensation method with a typical uncertainty of (1 to 2) %. The results of critical analysis of the previously reported ER data for nickel showed that the inconsistencies (deviations between various data sources) reached up to 10 %, which is five times higher than the typical uncertainty of the measurements. By critical analysis of the reported data, Bel'skaya and Peletsky [15,26] selected the primary consistent ER datasets for nickel. These data were recommended as a Russia reference standard. They proposed 5 reference correlations for various temperature ranges. The uncertainty of the recommended [15,26] ER data for nickel is 0.112 $\mu\Omega$·cm. Laubitz [24] measured the ER of nickel over the temperature range from (273 to 1273) K using the compensation (potentiometric) method with an uncertainty of (1.0 to 1.5) %. Excellent agreement within (0.3 to 1.4) % was found between the present measurements and the data reported by Laubitz [24] at high temperatures (above the Curie temperature). In the low-temperature range, the consistency of the measured ER data of nickel is within (5 to 7) %. The agreement of the Laubitz [24] results with the previously reported data by Bel'skaya and Peletsky

[15,25,26] is very good. The deviations are within 0.8 % at high temperatures (above 600 K) and 1.4 % at low temperatures.

Powell et al. [30] reviewed some reported ER data of Armco iron. Watson [19] measured the ER of two samples of Armco iron (99.834 mass %) in the temperature range from (78 to 1653) K at the National Bureau of Standards. Measurements were made using series calibrated standard resistors and a regulated dc power supply. The uncertainty of the ER measurements is 2 % or 0.1 $\mu\Omega$·cm. The data by Watson [19] agree with those reported by Powell et al. [20] within (1.0 to 1.5) % at high temperatures (above 273 K) and within about 6 % at low temperatures (below 273 K). The data reported by Laubitz [16] for Armco iron deviate from Watson's [19] measurements within 1 % at high temperatures. Deviations up to 5 % were found with the data by Fulkerson et al. [21] at low temperatures (below 323 K) and show systematic deviations within (1 to 3) % at high temperatures. The present ER measurements for iron agree with the Watson [19] measurements within (5 to 7) %. The present ER data for Armco iron are in agreement with the data of Arajs and Colvin [31] within 1 % at temperatures above 750 K while, at low temperatures (from room to 750 K), the deviations are large (up to 10 %). In general, the majority of previously reported ER data [16,17,19,20,28,31] for Armco iron are in satisfactory agreement with the present measurements within (3 to 8) % depending on the temperature range. The ER data reported by Kamalakar [7] are systematically lower than the present and other reported data [15,22,24,25] by 6.7 % in the critical region. Good agreement, within (2 to 3) %, was observed between the present and reported ER data [15,22,25]. Gumenuk and Lebedev [18] used the compensation (potentiometric) method to study the temperature dependence of ER of Armco iron (99.98 mass %) in the wide temperature range from (293 to 1723) K. The uncertainty of the measurements is 1.5 %. These data are systematically lower than the present and other reported [16,17,19,20,28] ER measurements by 21 % at low temperatures (below the Curie temperature) and by 10 % at high temperatures. The consistency between the Gumenuk and Lebedev [18] results and the data of Fulkerson et al. [21] is slightly better than the other reported data. The discrepancy is within (1 to 4) % at high temperatures (above 500 K) and up to (7 to 10) % at low temperatures (below 400 K). Deviations within 1 % at high temperatures (above 573 K) and (5 to 7) % at low temperatures were also observed between the present and Oleinikov [29] measurements. Thus, due to large inconsistencies, the scatter of the reported TEC data reaches up to (20 to 25) %, especially near the Curie temperature. A critical assessment of the previously reported ER data of Armco iron showed that most reported data deviate from each other within (0.5 to 1.0) %, although in some cases, the deviation is larger.

1.1.3 TEC and ER Near the Critical Point

Reported TEC and ER data of nickel and Armco iron near the phase transition temperature (Curie temperature) together with the present results are presented in Figs. 3 and 6. All these publications were discussed above (method and uncertainty of measurements, consistency, and the sample purity). As one can see, reported TEC data near T_C show large scatter. The uncertainty of the measurements and impurity effect near the Curie temperature is also large (up to 4 % to 5 %). The discrepancy between the

various reported data sources near the critical point is within 20 % to 25 %. Kamalakar and Raychaudhuri [32] studied the ER anomaly near the phase transition temperature T_C in bulk (diameter of 50 μm) and nickel nanowires (diameters less than 20 nm, purity 99.999 mass %). The measurements have been made in the temperature range from (4 to 675) K using the four-probe potentiometric method for bulk Ni and the pseudo-four-probe method for nanowires. The results were interpreted in terms of scaling theory (power law behavior, fluctuation theory of critical phenomena) including the noncritical (regular) part of the measured ER data. The measured ER data were used to accurately determine the values of theoretically important asymptotic (A_-, A_+) and nonasymptotic (D_-, D_+) critical amplitudes and the critical exponent (α). The authors studied how the values of the critical amplitudes (amplitude ratios) and the critical exponent (α) depend on the nanowire sizes (size effect on critical phenomena). The singularity of the temperature derivative ($\mathrm{d}\rho/\mathrm{d}T \propto t^{-\alpha}$) of the resistance for a bulk sample near T_C was observed. The results for the bulk sample are in good agreement with previous studies. The critical phenomena in Ni nanowires have also been studied in the work [33] by the same authors. They observed a decrease in the critical part (critical exponent, α) of the resistivity with nanowire diameter changes. Also, a decrease in the Curie temperature with nanowire size was observed. Kamalakar and Raychaudhuri [34] also reported the ER of a ferromagnetic Ni nanowire (diameter ranging from 55 nm to 13 nm). The measurement was made in the temperature range from (3 to 300) K. The results were interpreted in terms of the Bloch–Wilson function and the Debye temperature. The effect of the size of nanowires on the Debye temperature was studied. The authors found a strong suppression in the spin wave contribution to the resistivity of the magnetic nanowires as the diameter is decreased. Kraftmakher and Pinegina [35] also studied the critical anomaly of the ER of iron near the Curie temperature. They directly measured the temperature derivative of the ER, $\mathrm{d}\rho/\mathrm{d}T$. The measurements were made using the modulation method. The measured values of $\mathrm{d}\rho/\mathrm{d}T$ have been used to estimate the values of the asymptotic critical amplitudes (A_-, A_+) and the critical exponent (α). Major et al. [36] applied an optical dilatometer to measure the TEC of high-purity nickel near the Curie point. The measured values of the TEC were used to estimate the critical exponents and asymptotic critical amplitudes for $T < T_C$ and $T > T_C$.

2 Experimental

High-purity nickel (99.99 mass %) and ARMCO iron with 99.98 mass % purity (0.02 mass % of carbon and other impurities) have been used in this study. The details of the method and experimental apparatus, procedures, and uncertainty assessments for the simultaneous measurements of the electrical resistivity and TEC of solid materials were given in our previous publications [1,5]. A brief description will be given below. The measurements were made on cylindrical-shaped specimens with typical dimensions of 60 mm length and a diameter of 4.5 mm. The temperature dependence of the electrical resistivity $\rho(T)$ was measured with a standard dc four-probe potentiometric method. The thermal expansion coefficient was measured using the quartz dilatome-

ter technique. Both techniques for measurements of the electrical resistance and TEC were combined in the same apparatus (see details in our previous publication [1]). The main part of the apparatus consists of a quartz dilatometer, photo-electrical transducer, specimen, electrical circuitry for the stabilized current, and electrical circuitry for the temperature and electrical resistivity measurements. Measurements were performed in vacuum (the environment of the dilatometer can be either vacuum or any mixture of different gases). The combined expanded uncertainties of the electrical resistance $\rho(T)$ and thermal expansion coefficient $\beta(T)$ measurements at the 95 % confidence level with a coverage factor of $k = 2$ are estimated to be 0.5 % and (1.5 to 4.0) %, respectively. The method has been previously used for accurate measurements on other solid materials at high temperatures [1,4,5].

3 Results and Discussion

The measured ER and TEC data for nickel and ARMCO iron are presented in Table 2 and in Figs. 1, 2, 3, 4, 5, and 6 as a function of temperature together with the values reported by other authors. As can be noted, the present electrical resistivity and TEC data for Ni and ARMCO iron are in good agreement with previously reported data [6,8,9,14]. A detailed comparison of the present results with selected literature data is given above (see Sects. 1.1.1, 1.1.2). In general, the discrepancies between the present and most reliable reported data are within their experimental uncertainties (3 % to 5 % for TEC) and (0.5 to 1.0) % for resistivity.

3.1 Correlation Between the Electrical Resistivity and Thermal Expansion Coefficient

Figures 7 and 8 show the measured values of the total resistivity ρ for nickel and iron as a function of βT. Figure 8 also includes the data previously reported by Shmatko and Usov [22] for cobalt. As one can see from these figures, the experimental values of $\rho(T)$ are linearly related with the product of temperature T and TEC, i.e., $\beta T = \frac{T}{V}\left(\frac{\partial V}{\partial T}\right) = \frac{\partial \ln V}{\partial \ln T}$. The measured total electrical resistivity and TEC data above and below the Curie temperature ($T_C = 630$ K) for Ni can be described by simple linear relations

$$10^8\rho = -5.26 \times 10^{-8} + 10.245 \times 10^{-6}\beta T \quad \text{over the temperature range from (300 to 630.6) K} \tag{1}$$

$$10^8\rho = 19.65 \times 10^{-8} + 4.11 \times 10^{-6}\beta T \quad \text{over the temperature range from (800 to 1100) K} \tag{2}$$

Equations 1 and 2 reproduce measured values of resistivity within their experimental uncertainties. The Curie temperature of iron ($T_C = 1040$ K) is close to the structural (from bcc to a denser fcc structure) phase transition temperature ($T = 1184$K). Therefore, above 900 K the increase of the TEC due to the magnetic disordering is suppressed by the atomic structure densification [37]. For this reason, we have presented

Table 2 Measured values of electrical resistivity (ρ) and TEC (β) of nickel and Armco iron

T (K)	$\beta \times 10^6$ (K^{-1})	$\rho \times 10^8$ (Ω·m)	T, (K)	$\beta \times 10^6$ (K^{-1})	$\rho \times 10^8$ (Ω·m)
Nickel			*Armco iron*		
310	40.14	6.67	331.28	32.46	14.42
330	40.08	7.63	341.03	33.14	15.33
350	40.14	8.57	360.90	34.45	16.45
370	40.26	9.52	379.40	35.63	18.15
390	40.53	10.48	388.78	36.24	18.42
400	40.68	10.98	403.15	37.10	19.09
420	41.10	12.00	413.03	37.66	20.16
440	41.67	13.09	428.15	38.53	21.27
460	42.36	14.24	437.65	39.04	22.06
480	43.20	15.49	447.90	39.60	23.00
500	44.19	16.84	458.28	40.14	23.87
520	45.36	18.31	467.40	40.60	24.08
540	46.68	19.92	477.78	41.12	25.00
560	48.21	21.69	487.15	41.56	26.07
580	49.89	23.62	499.15	42.11	27.47
600	51.78	25.74	507.40	42.48	28.12
620	53.88	28.06	517.52	42.93	28.98
630	55.02	29.01	527.03	43.33	29.67
631	55.15	29.05	537.03	43.73	30.55
632	55.04	29.09	547.15	44.13	31.26
633	54.93	29.13	559.28	44.59	32.29
634	54.82	29.18	567.15	44.88	32.91
635	54.71	29.22	579.53	45.31	33.90
636	54.59	29.26	586.03	45.53	34.58
637	54.48	29.30	595.90	45.85	35.63
638	54.37	29.34	605.03	46.13	36.33
639	54.26	29.38	619.65	46.56	37.69
640	54.15	29.42	629.15	46.82	38.68
641	54.04	–	638.53	47.07	39.57
642	53.92	–	648.40	47.31	40.62
643	53.81	–	667.15	47.75	42.47
644	53.70	–	678.90	47.99	43.72
645	53.59	–	686.65	48.14	44.36
650	53.03	29.82	697.03	48.33	45.74
668	51.01	–	705.15	48.46	46.54
688	48.78	–	714.78	48.60	47.52
700	–	31.79	724.28	48.74	48.72
750	49.36	33.67	738.40	48.91	50.17
763	49.54	–	748.65	49.02	51.39

Table 2 continued

T (K)	$\beta \times 10^6$ (K^{-1})	$\rho \times 10^8$ (Ω·m)	T, (K)	$\beta \times 10^6$ (K^{-1})	$\rho \times 10^8$ (Ω·m)
800	50.58	35.47	755.40	49.09	52.21
820	50.97	36.16	772.40	49.22	54.33
840	51.42	36.84	780.03	49.27	55.06
850	–	37.17	791.90	49.32	56.30
860	51.90	37.50	798.78	49.34	57.72
880	52.41	38.16	809.90	49.36	59.16
900	52.98	38.79	818.40	49.37	60.44
920	53.58	39.42	827.15	49.37	61.63
940	54.21	40.02	837.90	49.34	62.89
950	–	40.32	846.78	49.31	64.11
960	54.90	40.62	855.90	49.27	65.34
980	55.05	41.20	865.90	49.21	66.93
1000	55.65	41.77	874.40	49.15	67.98
1020	56.37	–	883.90	49.06	69.59
1040	56.71	–	893.28	48.97	71.03
1050	–	43.12	902.40	48.88	72.01
1060	57.61	–	912.53	48.75	73.32
1080	58.48	–	920.40	48.64	75.18
1100	59.04	44.39	931.15	48.48	76.82
–	–	–	944.65	48.25	79.26
–	–	–	952.40	48.12	80.33
–	–	–	966.28	47.84	82.72
–	–	–	976.53	47.62	84.78
–	–	–	985.53	47.42	87.21
–	–	–	993.65	47.22	88.19
–	–	–	1004.90	46.94	90.01
–	–	–	1015.65	46.65	91.71
–	–	–	1023.53	46.43	94.16
–	–	–	1033.15	46.15	95.77
–	–	–	1041.65	45.89	98.43

the measured results of the resistivity and TEC for ARMCO iron in the ferromagnetic phase only, i.e., in the temperature range below 900 K (from 300 K to 900 K)

$$10^8\rho = -6.05 \times 10^{-8} + 1.2 \times 10^{-5}\beta T. \tag{3}$$

The universality of the linear relation between $\rho(T)$ and βT has been also theoretically and experimentally confirmed in our previous publications [1–5] for 30 metals and alloys in the temperature range from 0 K to the melting temperature. In the present work, we used this universal relation to predict some very important physical properties of materials.

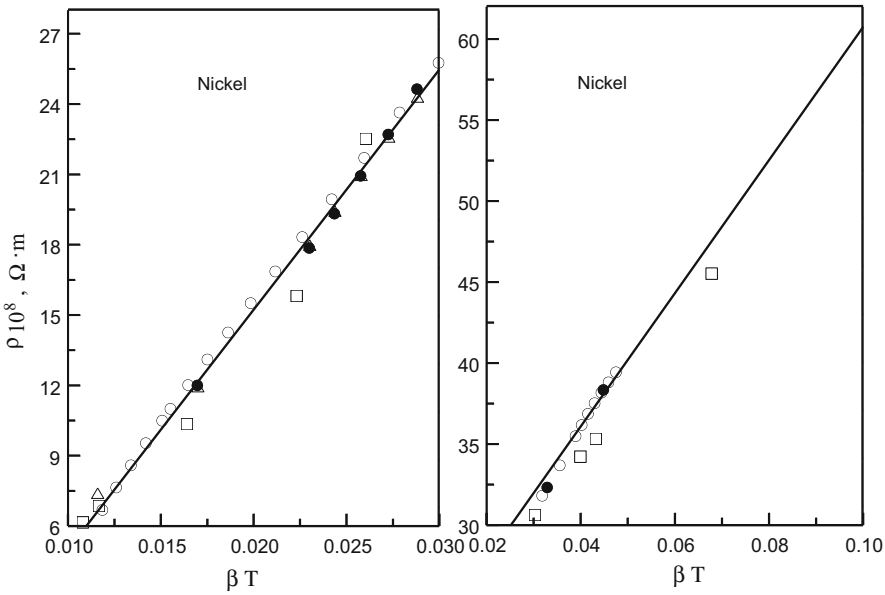

Fig. 7 Measured electrical resistivities for nickel as a function of TEC (from the present measurements) in the various temperature ranges. *Left* in the temperature range from (300 K to 620 K) and *Right* in the temperature range from (800 K to 1100 K). •—this work; □—Shmatko and Usov [22]; △—Bel'skaya and Peletsky [15]; *Solid lines* are calculated from correlation Eqs. 6 and 7

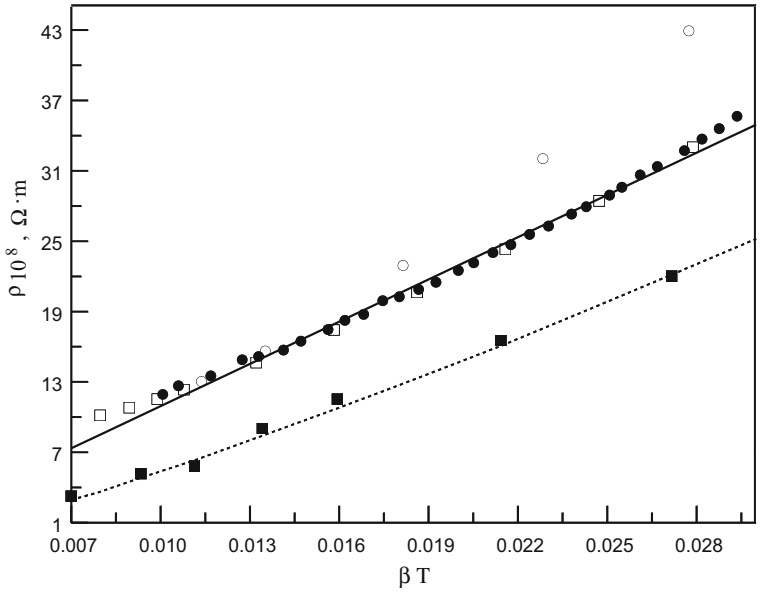

Fig. 8 Measured electrical resistivities for Armco iron and cobalt as a function of TEC (from the present measurements) in the temperature range from 300 K to 900 K. ○—Laubitz [16]; □—Gumenuk and Lebedev [18]; •—this work; ■—Shmatko and Usov [22] for cobalt; *Solid line* from correlation Eq. 3 for Armco iron

3.2 Distinct Resistivity Scattering Contributions (Phonon, Magnetic, and Residual) Extraction from the Measurements

The total measured electrical resistivity of ferromagnetic materials can be presented as a sum of three distinct contributions (Matthieseen relation) [38–43],

$$\rho\,(T) = \rho_{\mathrm{s}} + \rho_{\mathrm{ph}}\,(T) + \rho_{\mathrm{m}}\,(T)\,, \tag{4}$$

where ρ_{s} is the residual resistivity related with electron scattering by static defects, ρ_{ph} is the phonon scattering resistivity, and ρ_{m} is the magnetic contribution to the total measured resistivity. The value of ρ_{s} can be determined by extrapolation of the measured resistivity to 0 K and is generally independent of temperature [39]. Below the Curie temperature (T_{C}), the magnetic contribution, $\rho_{\mathrm{m}}(T)$, as well as $\rho_{\mathrm{ph}}(T)$, is a complex functions of temperature, because the $\rho_{\mathrm{m}}(T)$ and $\rho_{\mathrm{ph}}(T)$ anomaly increases with temperature due to violation of the long-range magnetic order. The magnetic contribution (scattering by paramagnons) $\rho_{\mathrm{m}}(T)$ in the paramagnetic phase is constant [39]. Usually, [37–47] the magnetic contribution $\rho_{\mathrm{m}}(T)$ is estimated by subtracting the lattice vibration contribution $\rho_{\mathrm{ph}}(T)$ from the total measured resistance $\rho(T)$. The phonon scattering resistivity $\rho_{\mathrm{ph}}(T)$ can be calculated using the Bloch–Grüneisen formula [40,48]. The measured resistivities are normalized by the extrapolating of the experimental values of $\rho(T \to 0)$ to zero temperature from the paramagnetic phase. Since the temperature dependence of the ER over the entire temperature range is nonlinear, the extrapolation to 0 K leads to a large uncertainty. On the other hand, the Bloch–Gruneisen equation was derived in the harmonic approximation (potential energy, $U \propto cr^2$, where r is the interatomic distance), i.e., without consideration of the interatomic distance changes with temperature, the anharmonicity effect, $U(T) \propto cr^2 - gr^3 - fr^4$. Thus, the Bloch–Grüneisen equation cannot be used for accurate quantitative estimates of the contribution of $\rho_{\mathrm{ph}}(T)$ at any temperature; and therefore, accurate estimates of the magnetic contribution, $\rho_{\mathrm{m}}(T)$. An accurate estimation (or correct separation) of the distinct resistivity contributions, $\rho_{\mathrm{ph}}(T)$ and $\rho_{\mathrm{m}}(T)$, in the total measured resistivity $\rho(T)$, is very complex and important for correct interpretations of the experimental results. It is physically clear that the TEC is directly related with the anharmonicity (interatomic distance changes r with temperature). The anharmonic effect governs the temperature behavior of both the resistivity and thermal expansivity of materials. Since the potential energy is a parabolic shape ($U \propto cr^2$) in the harmonic approximation, the average separation $\langle r(T)\rangle$ of the atoms is independent of temperature. As is well known, a true interatomic potential is not parabolic (parabolic only on the bottom of the potential well, for each equilibrium state defined by P, V, T). A consequence of this deviation from the harmonic potential is the fact that bonds can be dissociated at large separations. Higher up the potential well, the two sides are no longer symmetric. Thus, the interatomic potential can be represented by the anharmonic potential, $U(T) \propto cr^2 - gr^3 - fr^4$. The second term represents the asymmetry of the mutual repulsion, while the third term represents the softening of the vibrations at a large amplitude. The second term of the anharmonic potential leads to increases in the average $\langle r\rangle$ with increasing temperature, since at high temperatures, the asymmetry of the potential leads to a large value of the inter-

atomic separation distance. The increase of $\langle r(T)\rangle = \frac{3gkT}{4c^2}$ is the source of physical expansion in solids. If the unit cell of a solid has one side of dimension a, the thermal expansion in this direction, $\alpha_a = \frac{1}{a}\frac{\mathrm{d}a}{\mathrm{d}T}$ or $\alpha_a \propto \frac{1}{T}$.

At low temperatures ($T << T_\mathrm{D}$) the changes of the TEC with temperature is very large (more than 3 orders of magnitude), while at high temperatures, the temperature dependence of the TEC is weak (see Figs. 1, 3). Therefore, at low temperatures a significant change in the frequency spectrum (or energy distribution) of various atomic vibrations are related with the changes in the volume ($\Delta V/V \approx 10$ % or TEC) or interatomic distance. Usually, for theoretical calculations of the ER, the harmonic approximation is used to simplify the problem. In this case, the true deformation potential is replaced by the nonadiabatic potential which is given by the relative change of the amplitude of harmonic oscillations of the systems [48–50]. The assumption of the significance of anharmonicity at high amplitudes, i.e., at high temperatures, is the result of this approximation. A qualitative description of the temperature dependence of the kinetic coefficients without considering anharmonicity is possible only due to the fact that both the anharmonicity and amplitude of oscillations of atoms increase with temperature, $\langle r(T)\rangle = \frac{3gkT}{4c^2}$.

3.3 Theory

In our previous publications [1–5], we have showed that the electrical resistivity (phonon contribution to total resistivity, ρ_ph) is a linear function of TEC, βT, i.e.,

$$\rho_\mathrm{ph} = \rho^* \beta T, \tag{5}$$

where ρ^* is the characteristic resistivity of materials or $\rho_\mathrm{ph} = \rho^*$ at $\beta T = 1$. The validation of Eq. 5 has been theoretically and experimentally confirmed in our previous publications [1–5] for various materials (metals and alloys) in the temperature range from 0 K to the melting temperature. According to the theory developed in our previous publications [1–3], the value of the characteristic resistivity ρ^* can be estimated as follows:

$$\rho^* = \left(\frac{e\tilde{E}}{C_\mathrm{P}\tau_\varphi}\right), \tag{6}$$

where e, $\tilde{E}$, and C_P are the electron charge, internal electric field, and heat capacity, respectively; $\tau_\varphi = (\partial T/\partial\varphi)_\mathrm{P}$ is the change of the material's temperature due to release of the Joule heat under the influence of an external electrical field E. Equation 6 can be rewritten through microscopic parameters as [2,3]

$$\rho^* = 7.15 \times 10^{-10}\left(\frac{\mu^{8/3}T_\mathrm{D}^2}{\gamma^{5/3}Z^{1/3}}\right), \tag{7}$$

where μ, Z, and γ are the atom mass, valence, and density, respectively. The physical basis of Eq. 5 can be interpreted as follows. According to the virial theorem [49] for condensed matter,

$$\beta = \frac{1}{V}\left(\frac{\partial V}{\partial T}\right)_P = \frac{\partial E_{\text{total}}}{E_{\text{total}}\partial T}, \tag{8}$$

therefore,

$$\beta T = \frac{T}{V}\left(\frac{\partial V}{\partial T}\right)_{\text{P}} = \left(\frac{\partial \ln V}{\partial \ln T}\right)_{\text{P}} = \frac{\partial \ln E_{\text{total}}}{\partial \ln T}, \tag{9}$$

where $E_{\text{total}} = 2E_{\text{kin}} + E_{\text{pot}}$ is the total energy of the system. As can be noted, the total energy and its temperature change for each equilibrium state at constant pressure is a function of V and T. Since the volume of the system is $V \approx r^3$ (where r is the interatomic distance), the thermal expansion coefficient β reflects the changes of the interatomic distance (anharmonicity) with temperature, $\langle r(T)\rangle = \frac{3gkT}{4c^2}$ (see above, Sect. 3.2), while the temperature is responsible for increases of the disorder of thermal oscillations [2]. Therefore, the product βT determines (or is responsible) for the total electron scattering by the thermal excitations of the lattice (anharmonicity effect). Since the cross-section scattering of the elementary electronic excitations in ferromagnetic metals below T_{C} is formed by thermal excitation of atoms and the magnetic subsystem, it is physically reasonable (according to Eq. 9) to assume that the resistivity is also determined by the TEC, βT.

In the paramagnetic phase, the first term in Eq. 2, except for residual resistivity ρ_{s}, includes also the magnetic contribution [39]. The derived values of the slope coefficients in Eqs. 1 to 3, as well as in Eq. 5, are the theoretical limits of the ER (characteristic resistivity) which characterizes the effect of scattering of electrons on dynamic defects: phonons (ρ_{ph}) above T_{C} and phonons with a magnetic subsystem (ρ_{mph}) below T_{C}. According to the theory [51], ρ_{ph} and ρ_{mph} are determined by the constants of the deformation potentials of scattering for paramagnetic and ferromagnetic states. The values of the characteristic ER in the ferromagnetic and paramagnetic phases are inversely proportional to the corresponding characteristic frequencies: $(\nu_{\text{D}} + \nu_{\text{m}})$ and ν_{D}, where $\nu_{\text{D}} = k_{\text{B}}T_{\text{D}}/h$ and $\nu_{\text{m}} = k_{\text{B}}T_{\text{C}}/h$ [39] are the Debye frequency and the exchange interaction characteristic frequency for the (d-d interaction), respectively. Thus, the characteristic resistivities in paramagnetic and ferromagnetic phases can be expressed as follows:

$$\rho^*_{\text{ph}} = k\,\nu_{\text{D}}, \tag{10}$$

$$\rho^*_{\text{mph}} = k\,(\nu_{\text{D}} + \nu_{\text{m}})\,, \tag{11}$$

where k is the same constant for both paramagnetic and ferromagnetic states. The value of k for nickel can be determined based on the slope coefficient in Eq. 2 by taking into account Eq. 10. The value of the characteristic resistivity ρ^*_{mph} for Ni in the ferromagnetic phase calculated from Eq. 11 is $9.02 \times 10^{-6}\,\Omega\cdot$m. This value is close (difference is about 13 %) to the $10.24 \times 10^{-6}\,\Omega\cdot$m derived from Eq. 1 using the present ER experimental data. For calculations, we use the value of the Debye temperature of $T_{\text{D}} \approx 450$ K [52]. The same method has been used to estimate the value of ρ^*_{mph} for Fe and Co. This is additionally confirmation that the physical basis of the method is correct. For iron, the present experimental results, Eq. 3, shows that $\rho^*_{\text{mph}} = 1.20 \times 10^{-5}\,\Omega\cdot$m, while the value of ρ^*_{mph} estimated from Eq. 11 is $1.33 \times 10^{-5}\,\Omega\cdot$m. A very close result of $1.50 \times 10^{-5}\,\Omega\cdot$m has been found from the

data reported in Ref. [9,18]. The value of ρ^*_{mph} for Co calculated using Eq. 11 is 1.50×10^{-5} Ω·m, while the reported data [9,22] give the value of 1.63×10^{-5} Ω·m. As one can see, the agreement between the measured and predicted values of ρ^*_{mph} is sufficient, i.e., within the total uncertainty (about 10 %) of the reported values of ρ, β, T_{C} , and T_{D}, for these materials. Thus, this physically based technique can be used to accurately predict the contributions of the residual, phonon, and magnetic resistivities to the measured total resistivity, i.e., accurately separate the contributions of the various mechanisms which are determining the total experimentally observed electrical resistivity of the materials. Therefore, it is apparent that for 3d-metals, the temperature dependence of the ER caused by electron scattering in phonons and the magnetic subsystem at any temperatures can be calculated using

$$\rho_{\mathrm{mph}}\,(T) = \rho^*_{\mathrm{mph}}\beta T = \left(\rho^*_{\mathrm{ph}} + \rho^*_{\mathrm{m}}\right)\beta T = 4.2 \times 10^{-19}\,(\nu_{\mathrm{D}} + \nu_{\mathrm{m}})\,\beta \mathrm{T}. \qquad (12)$$

Since the magnetic contribution in the paramagnetic state is constant [39] above the Curie temperature T_{C} , Eq. 12 can be rewritten as

$$\rho\,(T) = 4.2 \times 10^{-19}\,(\nu_{\mathrm{m}}\beta_{\mathrm{c}}\mathrm{T_c} + \nu_{\mathrm{D}}\beta \mathrm{T})\,, \qquad (13)$$

where β_{c} is the value of TEC near T_{C}.
Figure 9 shows the temperature dependence of the values of the characteristic ER,

$$\rho^* = \frac{\rho(T) - \rho_{\mathrm{s}}}{\beta T}, \qquad (14)$$

for nickel in the ordered, disordered, and (two-phase) intermediate phases. As one can see from Fig. 9, the values of the characteristic ER ρ^* are almost independent of temperature. In the temperature range from (20 to 170) K, the magnetic contribution ρ_{m} to the total measured resistivity ρ is small. This means that the characteristic resistivity ρ^* is basically determined by electron—phonon scattering. The negligible small magnetic contribution $\rho_{\mathrm{m}}(T)$ to the total measured resistivity $\rho(T)$ was found by Kamalakar et al. [53]. In the temperature range from (170 to 620) K, the magnetic contribution $\rho_{\mathrm{m}}(T)$ increases; therefore, the value of the characteristic resistivity is higher, which is consistent with the results obtained from the present data, Eq. 1. The small differences between the characteristic resistivities obtained from the reported [7–15] and the present data, Eqs. 1 and 2, are within their uncertainties. The linear relationship between the ER and the TEC (βT) is also valid for the two-phase region. As one can see from Fig. 9, the characteristic ER in the intermediate (two-phase) region is about 5.8×10^{-5}Ω·m, which is lower than the value for the ferromagnetic phase, however, higher than for the paramagnetic phase. This was also confirmed in our previous studies for alloys (solid solutions) [5].

3.4 Relation Between the Resistivity and TEC for Nickel Nanowires

The developed semiempirical correlation (see above, Sect. 3.1) between ER $\rho(T)$ and TEC $\beta(T)$ have been applied for nickel wire and nanowire (see Fig. 10) ER data

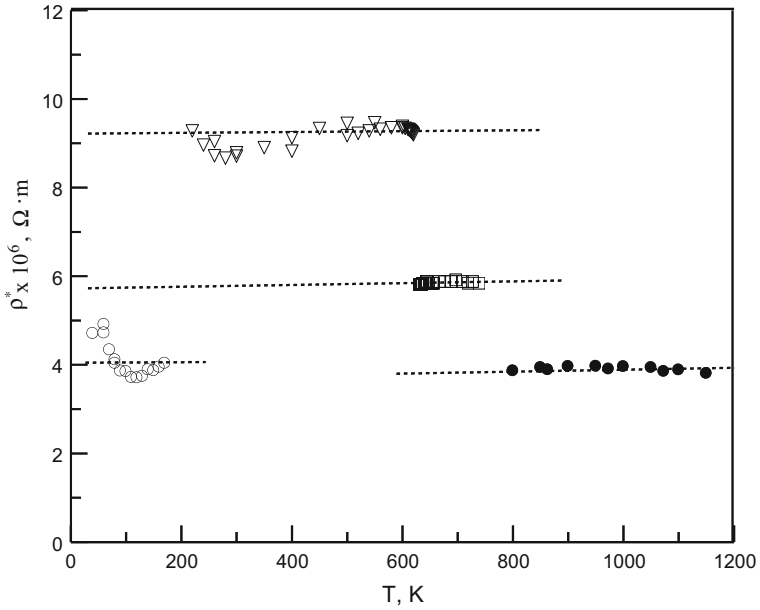

Fig. 9 Characteristic resistivity ρ^* versus temperature for nickel calculated from Eq. 14 in the ordered ◯—(20 K to 170 K), ▽—(170 K to 620 K); disordered •—(800 K to 1150 K) and intermediate (two-phase) □—(640 K to 780 K) phases

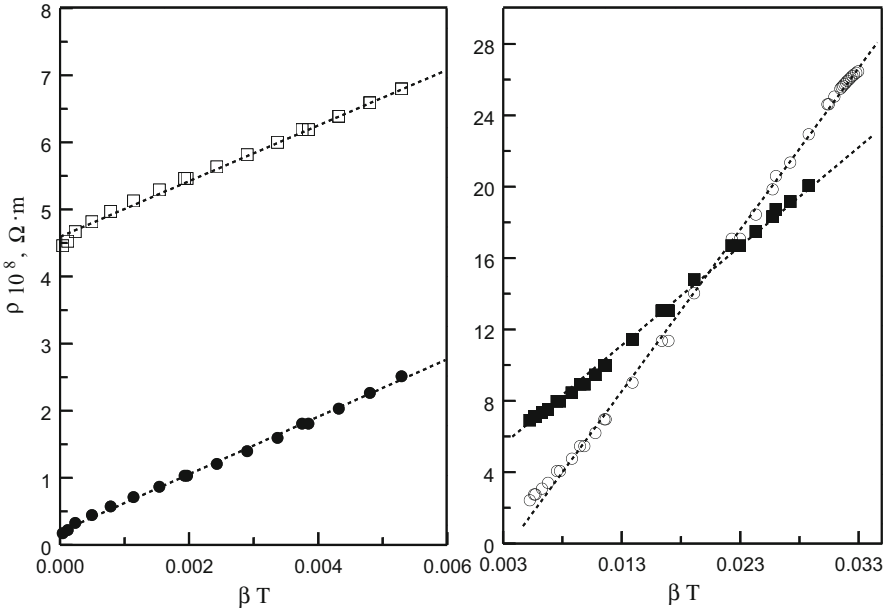

Fig. 10 Measured [7] electrical resistivities for nickel wire (50 μm) and nanowire (55 nm) as a function of TEC (from the present measurements) in the various temperature ranges. *Left* •—wire and □—nanowire; in the temperature range (35 K to170 K) and *Right* ◯—wire and ■—nanowire; in the temperature range (170 K to 580 K)

reported by Kamalakar et al. [7,53] and the present TEC data. The results can be represented as follows:

$$\rho_{\mathrm{b}} = 0.18 \times 10^{-8} + 4.27 \times 10^{-6} \beta T \quad \text{in the temperature range from (35 to 170) K} \tag{15}$$

$$\rho_{\mathrm{n}} = 4.50 \times 10^{-8} + 4.25 \times 10^{-6} \beta T \quad \text{in the temperature range from (35 to 170) K} \tag{16}$$

$$\rho_{\mathrm{b}} = -3.06 \times 10^{-8} + 8.98 \times 10^{-6} \beta T \quad \text{in the temperature range from (170 to 621) K} \tag{17}$$

$$\rho_{\mathrm{n}} = 3.54 \times 10^{-8} + 5.73 \times 10^{-6} \beta T \quad \text{in the temperature range from (170 to 580) K} \tag{18}$$

where ρ_{b} and ρ_{n} are the resistivities of the bulk and nanowire samples, respectively. For nanowires (55 nm), the correlation (Eq. 18) is given to 580 K, because the Curie temperature for nickel is 590 K [7] where the method is not applicable due to critical fluctuation effects. We used the same TEC data as in Fig. 1. As can be noted, in the temperature range from (35 to 160) K (Fig. 10, left), the characteristic resistivities for wire and nanowire are equal (i.e., the slopes of the $\rho_{\mathrm{b}} - \beta T$ and $\rho_{\mathrm{n}} - \beta T$ are almost the same, see also Eqs. 15 and 16). This means that the maximum phonon scattering cross section, which is defined by the value of ν_{D}, for wires and nanowires is very close to each other (almost the same). The discrepancy between the slopes of the $\rho_{\mathrm{b}} - \beta T$ and $\rho_{\mathrm{n}} - \beta T$ lines for wires and nanowires has been observed at temperatures above 170 K (see Fig. 10, right, and Eqs. 17 and 18). The characteristic resistivity of a nanowire (Eq. 18) is lower than for a wire (Eq. 17). This means that the magnetic contribution to the total ER in a nanowire becomes less than that in a wire. As was discussed in Ref. [53], this may be explained by the increase of the static disorder of spins in the nanowire due to the increases in the number of atoms on the surface (surface effect) with respect to those in the volume. Increases in the static disorder, as is well known [7], reduces the temperature coefficient of the resistivity.

3.5 Temperature Dependence of the s-d-Exchange Interaction Energy

The exchange interaction between the s- and d-electrons defines the anomaly of the temperature behavior of the ER due to magnetic ordering. The magnetic contribution of the ER, $\rho_{\mathrm{m}}(T)$, can be estimated based on Eq. 12 as follows:

$$\rho_{\mathrm{m}}(T) = \left(\rho^*_{\mathrm{mph}} - \rho^*_{\mathrm{ph}}\right) \beta T. \tag{19}$$

This allows determination of the temperature dependence of the s-d-exchange interaction energy of 3d-ferromagnets. Turov [46] proposed relation for the magnetic contribution $\rho_{\mathrm{m}}(T)$ of the total measured ER of the metallic ferromagnetic materials, based on the model s-d-exchange Hamiltonian as

$$\rho_{\mathrm{m}}(T) = \frac{3\pi m_{\mathrm{e}} V_0 \sigma \left|D\right|^2}{8e^2 \varepsilon_{\mathrm{F}} \hbar} \left(1 - \eta(T)^2\right), \tag{20}$$

where V_0 is the cell volume; e and σ- are the charge and spin of the electron, respectively; $\hbar = h/k$; h is the Plank constant; m_{e} is the electron mass; D is the paramagnetic energy of the s-d-exchange interaction; $\eta(T)$ is the relative spontaneous magnetization; and ε_{F} is the Fermi energy. To simplify the calculations, the author has assumed that D is a constant. From physical considerations [39,54] it follows that increases of the interatomic distance (anharmonicity effect) with temperature should lead to monotonic decreases of the energy. However, as will be shown below, the values of $D(T)$ for nickel, calculated from Eq. 20, using the derived values of $\rho_{\mathrm{m}}(T)$, extracted from the present $\rho(T)$ measurements (after separation of the phonon contribution ρ_{ph}), are functions of temperature (not constant). Equation 20 was theoretically confirmed and contains the well-defined empirical parameter $\eta(T)$, which is accounts for both the thermal disorder of spins and their disorder due to volume changes (TEC). The temperature dependence of the s-d-exchange interaction energy $D(T)$ can be estimated from Eq. 20, if the magnetic contribution $\rho_{\mathrm{m}}(T)$ is correctly extracted. Taking into account Eq. 19, Eq. 20 can be rewritten as

$$D(T) = K\sqrt{\frac{\rho_{\mathrm{m}}^* \beta T}{1 - \eta^2}}, \tag{21}$$

where the constant K can be estimate by microscopic parameters as follows:

$$K = \sqrt{\frac{8e^2 \varepsilon_{\mathrm{F}} \hbar}{3\pi m_{\mathrm{e}} V_0 \sigma}}. \tag{22}$$

The derived values of $D(T)$ using the present values of ρ_{m}^* and βT (see above) as a function of temperature for nickel can be presented (see Fig. 11) as an exponential function of temperature,

$$D(T) = D_0 \exp\left(-T/T_{\mathrm{C}}\right), \tag{23}$$

where $D_0 = 2.528$ eV. Equation 23 is consistent with Zener's [54] estimates within the high- and low- temperature limits. At the Curie point, $D(T_{\mathrm{C}}) = K\sqrt{\rho_{\mathrm{m}}^* \beta_{\mathrm{C}} T_{\mathrm{C}}} \approx 0.9$ eV. As was predicted by Zener [54], this value is approximately 2.2 times higher than for an isolated atom of Ni and about 6 times higher at $T \to 0$ K. This result is consistent with the exponential character of behavior of the exchange integral which decreases with increasing distance between the atoms below the Curie temperature, T_{C} [39].

In order to determine the temperature behavior of the s-d-exchange interaction energy for iron and cobalt, we have modified Eq. 20 using the experimentally derived Eq. 21 as follows:

$$\rho_{\mathrm{m}}^* \beta T = D_0^2 \mathrm{e}^{-\frac{2T}{T_{\mathrm{C}}}} \left(1 - \eta^2\right). \tag{24}$$

As can be noted from Fig. 12, the dependence of $\left(1 - \eta^2\right)$ *versus* $\beta T \exp(2T/T_{\mathrm{C}})$ for Ni, Fe, and Co is linear. This is additional confirmation of the exponential behavior of

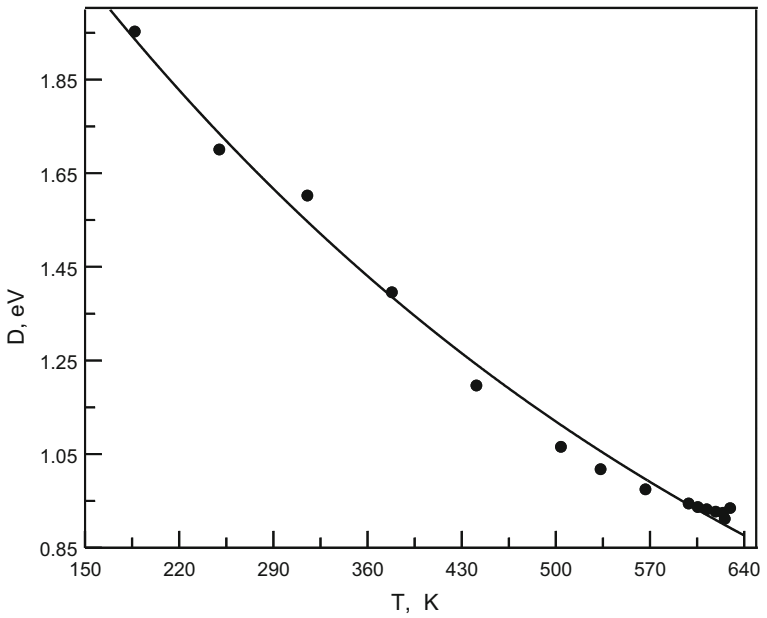

Fig. 11 Temperature dependence of $D(T)$ for nickel. *Solid line* is calculated from Eq. 23. *Symbols* are from the present experimental resistivity data

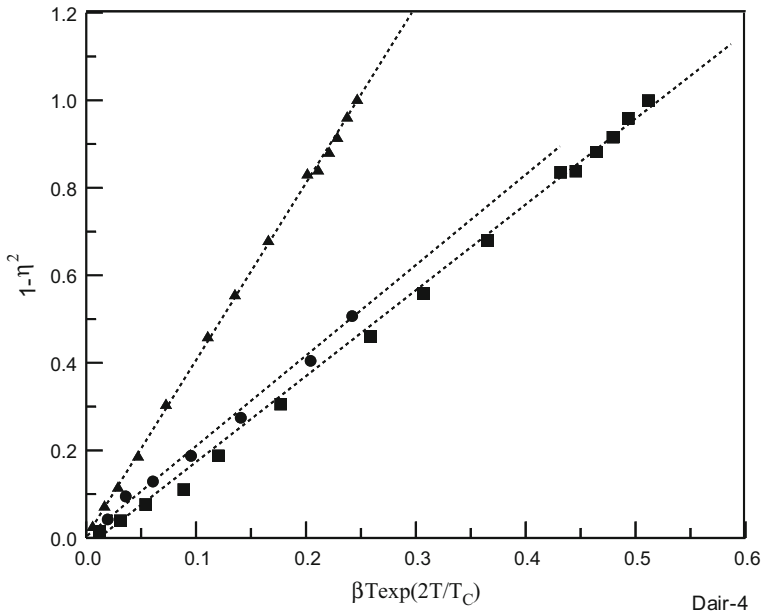

Fig. 12 $(1-\eta^2)$ versus $\beta T \exp(2T/T_C)$ for Ni (▲), Fe (●), and Co (■)

Table 3 Fermi energy, s-d and d-d-exchange interaction energy for the iron group metals

Element	ε_F (10^{-18} J)	T_C (K)	D_0 (eV)	D_0 (10^{-19} J)	E_{exc} (10^{-21} J)
Fe	1.77	1040	4.51	7.22	7.18
Co	1.86	1400	5.35	8.56	9.66
Ni	1.86	630	2.61	4.18	4.34

the temperature dependence of $D(T)$ for all of the 3-d-metals and allows an estimate of the value of D_0. The values of D_0 derived from Eq. 24 using the present experimental resistivity data for Ni, Fe, and Co are given in Table 3. The ratio of D_0 to the Fermi energy ε_F varies from 0.01 to 0.1. As can be noted from Table 3, the s-d-exchange interaction energy is below the Fermi energy ε_F, which is consistent with the results in Refs. [38,39]. However, unlike the d-d-exchange interaction energy, the s-d-exchange interaction energy is close to the Fermi energy, since, the d-electrons in the ions magnetize the s-electrons with energies close to ε_F. The interactions between d-electrons, with the exchange energy of $E_{exc} = k_B T_C$, is realized through all of the shared electrons. The values of E_{exc} for Fe, Co, and Ni are lower than D_0 by about two orders of magnitude.

4 Conclusions

In the present study, the electrical resistivity and thermal expansion coefficient of high-purity samples of nickel and ARMCO iron were simultaneously measured over the wide temperature range from (300 to 1100) K. A residual, phonon, and magnetic contribution extraction technique from the measured total electrical resistivity data was proposed. In order to understand the details of the temperature dependence of the ER of solid materials and correctly estimate the phonon scattering part of the measured total resistivity and the temperature dependence of the s-d-exchange interaction energy, the effect of anharmonicity should be taken into account. We experimentally found universal, physically based, semiempirical correlations between the kinetic coefficient (electrical resistance) and the thermodynamic (equilibrium) properties (thermal expansion coefficient) of solid materials. The correlation model has been used to estimate the properties of nanoscale (nanowires) materials. The derived correlation model provides an accurate (within their experimental uncertainty) estimate (prediction) of the values of the ER using the TEC measurements and vice versa. We showed that the value of the characteristic resistivity in the paramagnetic phase is proportional to the Debye frequency ν_D, while in the ferromagnetic phase, to the sum of the Debye frequency and the d-d-exchange interaction frequency, $(\nu_D + \nu_m)$. The exponential temperature dependence of the s-d-exchange interaction energy has been determined using the magnetic contribution extracted from the present measured resistivity data. The value of the s-d- exchange interaction energy is higher than the d-d-exchange interaction energy by two orders of magnitude, however, lower than the Fermi energy.

Acknowledgments I.M. Abdulagatov acknowledges the opportunity provided by the Applied Chemicals and Materials Division at the National Institute of Standards and Technology to work as a Guest Researcher at NIST during the course of this research. The authors also thank Dr. A.K Raychaudhuri and Dr. M.V. Kamalakar for providing the experimental resistivity data for nickel nanowires. This work was supported by the Russian Department of Science and Education, Projects Numbers 2560 and 16.1103.2014/K.

References

1. I.M. Abdulagatov, Zh.Kh. Murlieva, D.K. Palchaev, K.K. Kazbekov, M.M. Maangalov, J. Phys. Chem. Solids **68**, 1713 (2007)
2. D.K. Palchaev, Zh.Kh. Murlieva, K.K. Kazbekov, High Temp. **45**, 1 (2007)
3. K.K. Kazbekov, Zh.Kh. Murlieva, D.K. Palchaev, Tech. Phys. Lett. (Russian) **29**, 537 (2003)
4. Zh.Kh. Murlieva, D.K. Palchaev, E.D. Borzov, Russ. J. Technol. Phys. Lett. B **28**, 48 (2002)
5. Zh.Kh. Murlieva, M.E. Iskhakov, D.K. Palchaev, High Temp. **50**, 1 (2012)
6. R.N. Abdullaev, YuM Kozlovskii, R.A. Khairulin, S.V. Stankus, Int. J. Thermophys. **36**, 603 (2015)
7. M.V. Kamalakar, Ph.D. Thesis (Jadavpur University, Kolkata, 2009)
8. T.G. Kollie, Phys. Rev. B **1611**, 4872 (1977)
9. S.I. Novikova, *Thermal Expansions of the Solids* (Nauka, Moscow, 1974)
10. M.P. Arbuzov, I.A. Zelenkov, Phys. Met. Metall. **18**, 149 (1964)
11. Y. Tanji, J. Phys. Soc. Jpn. **31**, 1366 (1971)
12. H.W. Altman, T. Rubin, H.L. Johnston, *Coefficient of Thermal Expansion of Solids at Low Temperatures. III. The Thermal Expansion of Pure Metals, with the Data for Aluminum, Nickel, Titanium and Zirconium*, Cryogenic Laboratory Rep. OSU-TR-264-27. (Ohio State University, 1954)
13. M.E. Gurevich, L.N. Larikov, *An Automatic Dilatometer*, U.S. Air Force Report FTD-MT-24-893-71
14. G.K. White, Proc. Phys. Soc. **86**, 159 (1965)
15. E.A. Bel'skaya,V.E. Peletsky, *Nickel. The Electrical Resistivity in the Temperature Range 200–1500 K: Standard Reference Data* (GSSSD, Moscow, 1985)
16. M.I. Laubitz, Can. J. Phys. **38**, 887 (1960)
17. H.R. Shanks, A.H. Klein, G.C. Danielson, J. Appl. Phys. **38**, 2885 (1967)
18. V.S. Gumenuk, V.V. Lebedev, OMM (Russian) **8**, 223 (1959)
19. T.W. Watson, D.R. Flynn, H.E. Robinson, J. Res. NBS C **71**, 285 (1967)
20. R.W. Powell, R.P. Tye, M.J. Hickman, Int. J. Heat Mass Transf. **8**, 679 (1965)
21. W. Fulkerson, J.P. Moore, D.L. McElroy, J. Appl. Phys. **37**, 2639 (1966)
22. O.A. Shmatko, Y.A. Usov, *Electric and Magnetic Properties of Metals and Alloys* (Naukova Dumka, Kiev, 1987)
23. W. Wycisk, M. Feller-Kniepmeier, J. Appl. Phys. **48**, 839 (1977)
24. M.J. Laubitz, T. Matsumura, P.J. Kelly, Can. J. Phys. **54**, 92 (1976)
25. E.A. Bel'skaya, V.E. Peletsky, E.S. Amosovich, Thermophys. Prop. Subst. Mater. **13**, 125 (1985)
26. E.A. Bel'skaya, V.E. Peletsky, Teplofiz. Vys. Temp. **19**, 525 (1981)
27. A.F. Zverev, A.I. Kovalev, A.V. Logunov, Inzh. Fiz. Zh. (Russian) **24**, 164 (1973)
28. R.W. Powell, Proc. Phys. Soc. **46**, 659 (1934)
29. P.P. Oleinikov, High Temp. **19**, 533 (1974)
30. R.W. Powell, M.J. Hickman, R.P. Tye, M.J. Woodman, in *International Research on Thermodynamics and Transport Properties* (ASME, AP, New York, 1962)
31. S. Arajs, R.V. Colvin, Phys. Status Solidi **6**, 797 (1964)
32. M.V. Kamalakar, A.K. Raychaudhuri, Phys. Rev. B **82**, 195425 (2010)
33. M.V. Kamalakar, A.K. Raychaudhuri, J. Nanosci. Nanotechnol. **9**, 5248 (2009)
34. M.V. Kamalakar, A.K. Raychaudhuri, Phys. Rev. B **79**, 205417 (2009)
35. YaA Kraftmakher, TYu. Pinegina, Sov. Phys.-Solid State **16**, 132 (1974)
36. J. Major, F. Mezei, E. Nagy, E. Svab, G. Tichy, Phys. Lett. A **35**, 377 (1971)
37. E.A. Turov, Bull. Russian Acad. Sci. Phys. **194**, 474 (1955)
38. S.V. Vonsovskij, YuA Isyumov, Physics-Uspekhi **77**, 377 (1962)
39. S.V. Vonsovskij, *Magnetism*, 1st edn. (Nauka, Moscow, 1971)
40. F.J. Blatt, *Physics of Electronic Conduction in Solids* (McGraw-Hill, Michigan, 1968)
41. P. Stoch, J. Pszczoła, P. Guzdek, J. Chmist, W. Bodnar, A. Jabło'nska, J. Suwalski, A. Pa'nta, J. Alloys Compd. **392**, 62 (2005)

42. A.M. Pereira, J.P. Araújo, J.R. Peixotoet, Phys. Rev. B **83**, 144117–1 (2011)
43. M. Bednarski, J. Chmist, P. Stochand, J. Pszczoła, J. Phys. Scr. **85**, 035703 (2012)
44. A.A. Yudin, Bull. Moscow State Univ. (Phys.) **4**, 89 (1958)
45. E.A. Turov, Bull. Russian Acad. Sci. Phys. **194**, 462 (1955)
46. E.A. Turov, Met. Metallogr. **62**, 203 (1958)
47. A.A. Yudin, Bull. Moscow State Univ. Phys. **3**, 81 (1958)
48. J.M. Ziman, *Principles of the Theory of Solids*, 2nd edn. (Cambridge University Press, Cambridge, 1972)
49. J.C. Slater, *Insulators, Semiconductors and Metals* (McGraw-Hill Book Company, Inc., New York, 1967)
50. V.F. Gantmakher, *Electrons in the Disordered Media* (Fizmatlit, Moscow, 2003)
51. V.F. Gantmakher, I.B. Levinson, *Scattering of Charge Carriers in Metals and Semiconductors* (Nauka, Moscow, 1984)
52. C. Kittel, *Introduction to Solid State* (Wiley, New York, 1978)
53. M.V. Kamalakar, A.K. Raychaudhuri, X. Wei, J. Teng, P.D. Prewett, Appl. Phys. Lett. **95**, 013112 (2009)
54. C. Zener, Phys. Rev. **814**, 440 (1951)